Carbon Monoxide Production during the Oxygenation of Cobalt Complexes of Linear Tetrapyrroles. Formation and Characterization of Co^{II}(tetraethylpropentdyopent anion)$_2$

Richard Koerner, Marilyn M. Olmstead, Pamela M. Van Calcar, Krzysztof Winkler, and Alan L. Balch*

Department of Chemistry, University of California, Davis, California 95616

Received October 10, 1997

In the presence of dioxygen, four cobalt complexes of linear tetrapyrroles, Co(OEB) (OEB is the trianion of octaethylbiliverdin), $[Co^{II}(OEBOx)]I_3$ (OEBOx is the monoanion of the oxidized form of octaethylbiliverdin), Co^{II}(OEFB) (OEFB is the octaethylformylbiliverdin dianion), and Co^{II}(OEBOMe) (OEBOMe is the dianion of octaethylmethoxybiliverdin) form the bischelate cobalt(II) complex of the anionic dipyrrole, tetraethylpropentdyopent anion, $Co^{II}(TEPD)_2$. Both carbon monoxide and carbon dioxide are formed when $Co^{II}(TEPD)_2$ is produced by the thermal reactions between Co^{II}(OEFB) or Co(OEB) and O_2. Three different crystal morphologies of Co^{II}-$(TEPD)_2$ have been analyzed by single-crystal X-ray diffraction. In each case the cobalt atom is coordinated by four nitrogen atoms of the two propentdyopent ligands in a pseudotetrahedral fashion. In each morphology, a common tab/slot intermolecular C−H···O hydrogen bond interaction that involves the methine C−H unit and two adjacent C−H units of the flanking ethyl groups and the lactam oxygen atom is found. These interactions connect pairs of molecules into extended chains. $Co^{II}(TEPD)_2$ has been characterized spectroscopically (UV−vis and NMR) and electrochemically.

Introduction

Propentdyopents, **1**, are dipyrroles that are formed under several physiological conditions and are readily identified in urine. In a reaction discovered by Stokvis in 1870, the addition of a reductant to urine can produce a red solution,[1] which is more apparent in the urine of icteric neonates treated with blue light irradiation and patients with hepatitis.[2] The mechanism of the Stokvis reaction has received previous attention and involves the reduction of the colorless propentdyopent, **1**, to the corresponding red pentdyopent, **2**.[3] Studies of the reduction

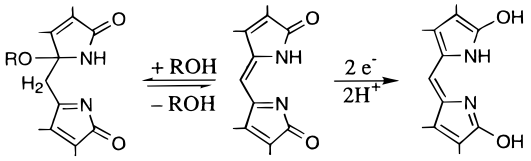

3 **1** **2**

process have shown that it occurs stepwise, with an intermediate radical form readily detectable by EPR spectroscopy. Thus the propentdyopent/pentdyopent couple is analogous to the quinone/hydroquinone couple. Various synthetic routes to propentdyopents have been reported.[3d,4] In the presence of water or alcohols, propentdyopents undergo reversible addition reactions to form the adduct **3**.

Biological routes to the formation of propentdyopents involve degradation of heme and oxidation of bilirubin,[5,6] which is also a heme degradation product. Scheme 1 shows some pertinent biological reactions. The reactivity of heme oxygenase produces specific cleavage at the α methine position to release the methine carbon atom as carbon monoxide, free iron ion, and biliverdin.[7] Carbon monoxide's role as a putative neurotransmitter has been recently discussed.[8] After heme cleavage, biliverdin is subsequently reduced to bilirubin, the yellow pigment responsible for human jaundice, by biliverdin reductase. Bilirubin is oxidized to a mixture of propentdyopents and biliverdin by the copper-containing enzyme, bilirubin oxidase.[9] Biliverdin itself has been shown to have antioxidant and antiviral properties.[10] An alternate path of heme degradation is found in the NADPH dependent reactions of cytochrome P-450 reductase or cyto-

(1) Stokvis, B. J. *Maandbl. Natuurwetenschappen* **1870**, *5*, 65. Stokvis, B. J. *Maandbl. Natuurwetenschappen* **1871**, *2*, 17.
(2) (a) Lucey, J.; Ferreiro, M.; Hewitt, J. *Pediatrics* **1968**, *41*, 1047. (b) Porto, S. O.; Hsia, D. Y.-Y. *J. Pediatr.* **1969**, *74*, 812. (c) Moravec, M. *Acta Hepato-Splenol.* **1971**, *18*, 402.
(3) (a) Von Dobeneck, H. *Hoppe-Seyler's Z. Physiol. Chem.* **1941**, *269*, 268. (b) Von Dobeneck, H.; Brunner, E.; Deffner, U. *Z. Naturforsch.* **1967**, *10*, 1005. (c) Von Dobeneck, H.; Brunner, E. Z. *Klin. Chem. Klin. Biochem.* **1969**, *7*, 113. (d) Von Dobeneck, H. In *The Porphyrins*; Dolphin, D., Ed.; Academic Press: New York, 1979; Vol. 6, p 651.
(4) (a) Bonnett, R.; Dimsdale, M. J.; Stephenson, G. F. *J. Chem. Soc., Perkin Trans. 1*, **1987**, 439. (b) Bonnett, R.; Chaney, B. D. *J. Chem. Soc., Perkin Trans. 1*, **1987**, 1063. (c) Bonnett, R.; Ioannou, S.; Swanson, F. J. *J. Chem. Soc., Perkin Trans. 1*, **1989**, 711.
(5) (a) Kutty, R. K.; Maines, M. D. *Biochem. J.* **1987**, *246*, 467. (b) Schaefer, W. H.; Harris, T. M.; Guengerich, F. P. *Biochemistry* **1985**, *24*, 3254. (c) Yoshinaga, T.; Sassa, S.; Kappas, A. *J. Biol. Chem.* **1982**, *257*, 7794. (d) Guengerich, F. P. *Biochemistry* **1978**, *17*, 3633.
(6) (a) Bonnett, R.; Stewart, J. C. M. *Chem. Commun.* **1972**, 596. (b) Lightner, D. A.; Quistad, B. *FEBS Lett.* **1973**, *25*, 94. (c) Lightner, D. A.; Linnane, W. P.; Ahlfors, C. E. *Pediatr. Res.* **1984**, *18*, 696.
(7) (a) O'Carra, P. In *Porphyrins and Metalloporphyrins*; Smith, K. M., Ed.; Elsevier: New York, 1975; p 123. (b) Schmid, R.; McDonagh, A. F. In *The Porphyrins*; Dolphin, D., Ed.; Academic Press: New York, 1979; Vol. 6, p 258. (c) Brown, S. B. In *Bilirubin*; Heirwegh, K. P. M., Brown, S. B., Eds.; CRC Press, Inc.: Boca Raton, FL, 1982; Vol. 2, p 1. (d) Bissell, D. M. In *Liver: Normal Function and Disease, Vol. 4, Bile Pigments and Jaundice*; Ostrow, J. D., Ed.; Marcel Decker, Inc.: New York, 1986; p 133. (e) Maines, M. D. *Heme Oxygenase: Clinical Applications and Functions*; CRC Press: Boca Raton, FL, 1992. (f) Chang, C. K.; Avilés, G.; Bag, N. J. *J. Am. Chem. Soc.* **1994**, *116*, 12127.
(8) Verma, A.; Hirsch, D. J.; Glatt, G. E.; Ronnett, G. V.; Snyder, S. H. *Science* **1993**, *259*, 381.

S0020-1669(97)01265-2 CCC: $15.00 © 1998 American Chemical Society
Published on Web 02/18/1998

Scheme 1

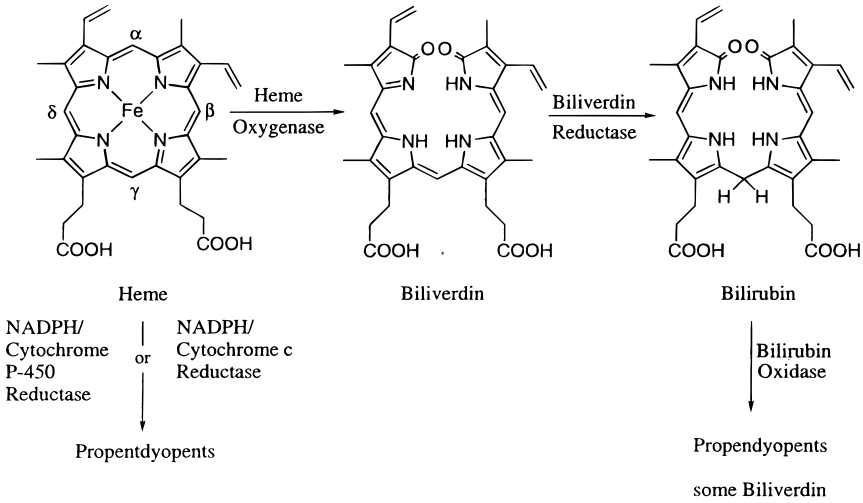

chrome *c* reductase.[5] A mixture of the four possible propentdyopents is formed in these pathways where the heme cleavage is nonspecific with cleavage at any of the four methine positions.

Several chemical routes to propentdyopent formation are relevant to these biological reactions. Cleavage of hemes by hydrogen peroxide yields four propentdyopents along with hematinic acid and methyl vinyl maleimide.[11] Propentdyopents are also formed in the reaction of bilirubin with superoxide anion radical generated by xanthine oxidase.[12] Finally, this laboratory has shown that copper(octaethylbiliverdin), Cu(OEB), slowly oxidizes in air to form $Cu^{II}(TEPD)_2$, the only crystallographically characterized transition metal complex of a propentdyopent.[13]

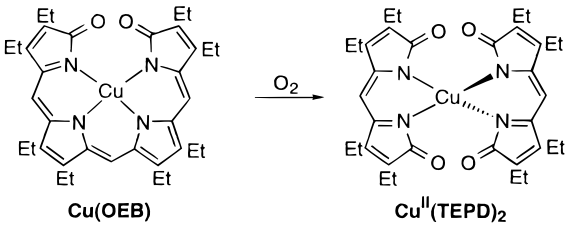

Here we describe a series of oxidative reactions which produce the cobalt analogue of $Cu^{II}(TEPD)_2$ along with carbon monoxide and carbon dioxide.

Results

Synthesis and Characterization of $Co^{II}(TEPD)_2$. Chemical routes to the formation of cobalt(II) (tetraethylpropentdyopent anion), $Co^{II}(TEPD)_2$, are summarized in Scheme 2. $Co^{II}(TEPD)_2$ was produced in good yield (66%) by the UV photooxidation of a benzene solution of $Co^{II}(OEFB)$.[14] Similarly, photooxidation of Co(OEB)[15] produces $Co^{II}(TEPD)_2$ in 9% yield. Alternatively, when a toluene solution of $Co^{II}(OEFB)$ or Co(OEB) is heated at 90 °C under a dioxygen atmosphere, $Co^{II}(TEPD)_2$ is produced in 10−16% yield. The product, $Co^{II}(TEPD)_2$, was crystallized from the reaction solution by the addition of *n*-hexane and collected by filtration. Additionally crystals of $Co^{II}(TEPD)_2$ formed during attempts to grow crystals of $[Co^{II}(OEBOx)]I_3$[16] and of $Co^{II}(OEB-OMe)$[17] in the presence of atmospheric oxygen. Crystals of $Co^{II}(TEPD)_2$ are soluble only to the millimolar level in chloroform, dichloromethane,

Scheme 2

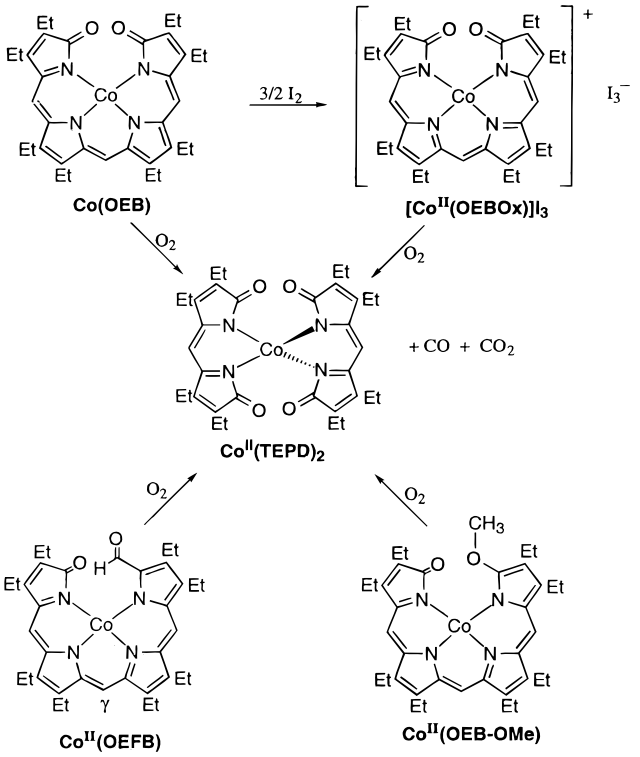

(9) (a) Stocker, R.; Yamamoto, Y.; McDonagh, A. F.; Glazer, A. N.; Ames, B. N. *Science*, **1987**, *235*, 1043. (b) Nakagami, T.; Taji, S.; Takahashi, M.; Yamanishi, K. *Microbiol. Immunol.* **1992**, *36*, 381. (c) Mori, H.; Otake, T.; Morimoto, M.; Ueba, N.; Kunita, N.; Nakagami, T.; Yamasaki, N.; Taji, S. *Jpn. J. Cancer Res.* **1991**, *82*, 755.

(10) (a) Yokosuka, O.; Billing, B. *Biochim. Biophys. Acta* **1987**, *923*, 268. (b) Cardenas-Vazquez, R.; Yokosuka, O.; Billing, B. H. *Biochem. J.* **1986**, *236*, 625.

(11) Schaefer, W. H.; Harris, T. M.; Guengerich, F. P. *Biochemistry*, **1985**, *24*, 3263.

(12) Itoh, S.; Gotani, T.; Imai, T.; Isobe, K.; Onishi, K.; Onishi, S. *Photomed. Photobiol.* **1995**, *17*, 55.

(13) Balch, A. L.; Mazzanti, M.; Noll, B. C.; Olmstead, M. M. *J. Am. Chem. Soc.* **1993**, *115*, 12206.

(14) Koerner, R.; Olmsted, M. M.; Ozaroski, A.; Phillips, S. L.; Van Calcar, P. M.; Winkler, K.; Balch, A. L. *J. Am. Chem. Soc.* **1998**, *120*, 1274.

(15) Balch, A. L.; Mazzanti, M.; Noll, B. C.; Olmstead, M. M. *J. Am. Chem. Soc.* **1994**, *116*, 9114.

(16) (a) Attar, S.; Balch, A. L.; Van Calcar, P. M.; Winkler, K. *J. Am. Chem. Soc.* **1997**, *119*, 3317. (b) Attar, S.; Balch, A. L.; Van Calcar, P. M.; Winkler, K. *Chem. Commun.* **1997**, 1115.

(17) Latos-Grażyński, L.; Johnson, J.; Attar, S.; Olmstead, M. M.; Balch, A. L. *Inorg. Chem.*, submitted.

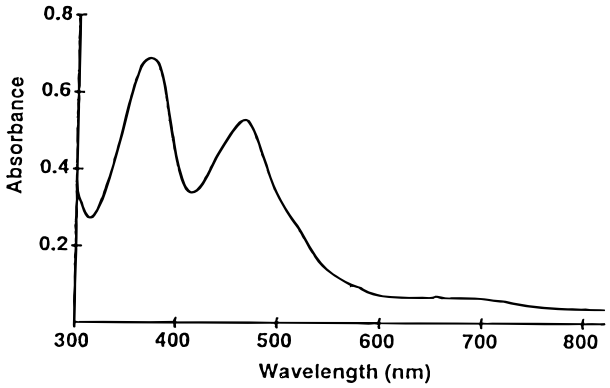

Figure 1. Electronic absorption spectra [λ_{max}, nm (ϵ, cm^{-1}·L·mol^{-1})] of a methylene chloride solution of $Co^{II}(TEPD)_2$: 368 (4.1 × 10^3), 464 (2.9 × 10^3), 548 sh (1.1 × 10^3), 662 (4.5 × 10^2).

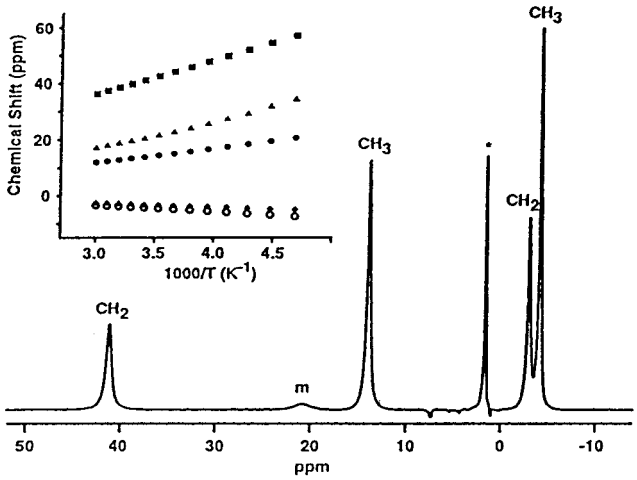

Figure 2. The 300 MHz ^{1}H NMR spectrum of $Co^{II}(TEPD)_2$ in chloroform-*d* at 23 °C. The spectrum was collected under inversion−recovery conditions (τ = 100 ms). Resonance labels: CH_2, methylene; CH_3, methyl; m, meso; "*" denotes residual water in the solvent. The inset shows the chemical shift dependence upon T^{-1} for $Co^{II}(TEPD)_2$ in chloroform-*d*.

benzene, and toluene and produce red-brown solutions. The characteristic UV−vis spectrum of $Co^{II}(TEPD)_2$ in dichloromethane solution is shown in Figure 1. A similar UV−vis spectrum (λ_{max}, 376, 466, 662 nm) has been obtained from a pyridine solution. Thus the complex does not readily accept additional ligands. Both as a solid and in solution, $Co^{II}(TEPD)_2$ is air and light stable.

The thermal oxidation of Co^{II}(OEFB) and Co(OEB) produce quantities of both carbon monoxide and carbon dioxide. These two oxidation products were detected by infrared spectroscopic analysis of the gases above the reaction mixture. Unfortunately it was not possible to examine the formation of carbon monoxide and carbon dioxide in the photolytic reactions, because photooxidation of benzene or toluene produces detectable amounts of CO under the reaction conditions used to produce $Co^{II}(TEPD)_2$. However, a toluene blank subjected to the thermal oxidation procedure does not produce detectable quantities of CO or CO_2.

Figure 2 shows the ^{1}H NMR spectrum of $Co^{II}(TEPD)_2$ in chloroform-*d* at 23 °C. The spectrum was collected under inversion−recovery conditions where diamagnetic resonances are inverted or diminished in intensity, and in this figure the inverted resonance due to residual protons from chloroform-*d* has been truncated. The assignments shown in the figure are based upon relative integrated intensities measured for the

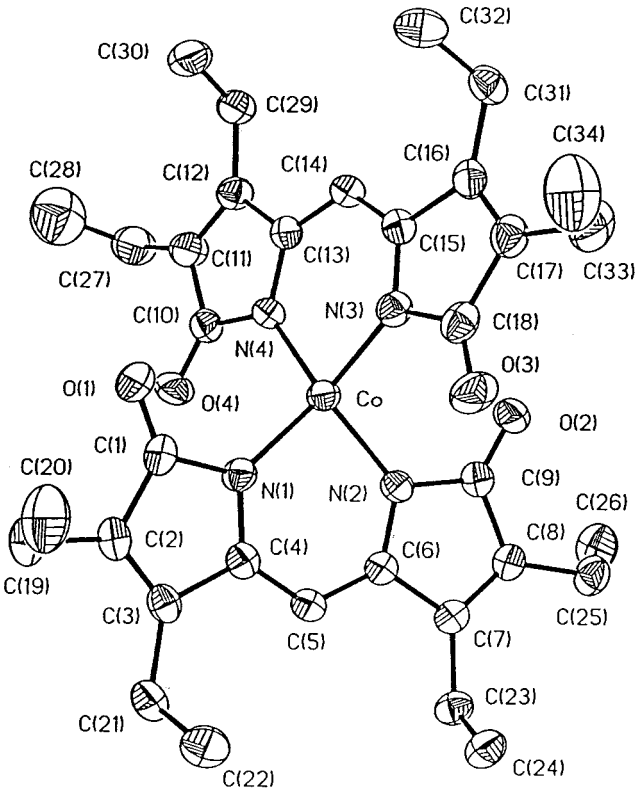

Figure 3. Perspective view of $Co^{II}(TEPD)_2$·0.5C_6H_6 with 50% thermal contours for all atoms. The benzene solvate has been omitted for clarity.

complex under non inversion−recovery conditions. The inset in Figure 2 shows the chemical shift dependence upon T^{-1} for $Co^{II}(TEPD)_2$. In general the resonances obey the Curie law, but the plot for the chemical shift of the meso resonance shows some curvature. In chloroform-*d* solution the magnetic susceptibility of $Co^{II}(TEPD)_2$ was determined to be 3.9 μ_B at 23 °C. This is consistent with the presence of high-spin ($S = {}^3/_2$) cobalt(II) in the complex.

Crystal and Molecular Structure of $Co^{II}(TEPD)_2$. Suitable crystals for X-ray diffraction were grown as follows: a red parallelepiped of $Co^{II}(TEPD)_2$·0.5C_6H_6 was obtained by the slow diffusion of *n*-hexane into a benzene solution of $Co^{II}(TEPD)_2$; a purple block of $Co^{II}(TEPD)_2$·CH_2Cl_2 was obtained from slow diffusion of *n*-pentane into a dichloromethane solution of [Co^{II}(OEBOx)]I_3; a brown plate of $Co^{II}(TEPD)_2$·2$CHCl_3$ was obtained by the slow diffusion of *n*-hexane into a chloroform solution of Co^{II}(OEB−OMe). The variation in color between these forms is ascribed to differences in crystal size and shape which effect the relative transmission and reflection of the crystals. The crystals of $Co^{II}(TEPD)_2$·CH_2Cl_2 and $Co^{II}(TEPD)_2$·2$CHCl_3$ grew under aerobic conditions which indicates that [Co^{II}(OEBOx)]I_3 and Co^{II}(OEB−OMe), like Co^{II}(OEFB), are air sensitive and oxidatively degrade to form a common product, $Co^{II}(TEPD)_2$.

A perspective view of the $Co^{II}(TEPD)_2$ molecule in $Co^{II}(TEPD)_2$·0.5C_6H_6 is shown in Figure 3. Coordination about cobalt in the other two crystalline variants is similar. In $Co^{II}(TEPD)_2$·CH_2Cl_2 the cobalt complex has 2-fold rotational symmetry that is crystallography imposed while in the other two structures there is no crystallographic symmetry to the complex. Table 1 presents a comparison of selected bond distances and angles for the three different structures.

The overall geometry of the complexes in all three forms is approximately D_2 and deviates significantly from D_{2d} symmetry

Table 1. Selected Bond Lengths (Å) and Angles (deg) for $Co^{II}((TEPD)_2 \cdot 0.5C_6H_6$, $Co^{II}((TEPD)_2 \cdot CH_2Cl_2$, and $Co^{II}((TEPD)_2 \cdot 2CHCl_3$[a]

	$Co^{II}(TEPD)_2 \cdot 0.5C_6H_6$	$Co^{II}(TEPD)_2 \cdot CH_2Cl_2$	$Co^{II}(TEPD)_2 \cdot 2CHCl_3$
	Bond Lengths (Å)		
Co−N(1)	1.969(2)	1.981(7)	1.980(6)
Co−N(2)	1.979(2)	1.971(11)	1.974(6)
Co−N(3)	1.970(3)		1.985(6)
Co−N(4)	1.978(2)		1.969(6)
O(1)−C(1)	1.216(4)	1.18(2)	1.201(9)
O(2)−C(9)	1.213(3)	1.218(11)	1.223(9)
O(3)−C(18)	1.210(4)		1.215(9)
O(4)−C(10)	1.215(4)		1.221(9)
	Bond Angles (deg)		
N(1)−Co−N(2)	91.58(10)	91.6(4)	91.2(2)
N(1)−Co−N(3)	124.57(10)	129.2(4)	133.1(2)
N(1)−Co−N(4)	113.35(10)	110.2(4)	108.6(2)
N(2)−Co−N(3)	110.70(10)		110.1(2)
N(2)−Co−N(4)	128.08(10)	128.4(5)	127.2(2)
N(3)−Co−N(4)	92.08(10)		92.5(2)

[a] The numbering schemes used in all three structures are related.

that would be present if the planes of the two ligands were perpendicular. The cobalt atom has four-coordinate, nonplanar geometry with Co−N bond distances in a narrow range, 1.969(2)−1.985(6) Å. These distances are consistent with those seen in other nonplanar, four-coordinate cobalt(II) complexes with CoN_4 coordination spheres. The average Co−N distance for 12 compounds in the Cambridge Crystallographic Data Base (CCDB) with CoN_4 coordination and a bischelate structure is 1.96 Å. The propentdyopent ligands themselves are nearly planar. The individual mean deviation from the plane defined by the two nitrogen atoms and the nine carbon atoms of the ligand core are 0.07 Å for the N(1)−N(2) ligand and 0.03 Å for the N(3)−N(4) in $Co^{II}(TEPD)_2 \cdot 0.5C_6H_6$; 0.04 Å in $Co^{II}(TEPD)_2 \cdot CH_2Cl_2$; 0.03 for both ligands in $Co^{II}(TEPD)_2 \cdot 2CHCl_3$. The dihedral angles between the two ligand planes are 74.8° in $Co^{II}(TEPD)_2 \cdot 0.5C_6H_6$, 67.5° in $Co^{II}(TEPD)_2 \cdot CH_2Cl_2$, and 69.3° in $Co^{II}(TEPD)_2 \cdot 2CHCl_3$. For the 12 compounds in the CCDB with CoN_4 coordination and a bischelate geometry, the average analogous dihedral angle is 80.5°.

The geometry of $Co^{II}(TEPD)_2$ is closely related to that of nickel (3,3′,5,5′-tetramethyldipyrromethane), $Ni^{II}(TMDP)_2$, which

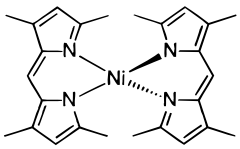

$Ni^{II}(TMDP)_2$

also has approximate D_2 symmetry with an angle of 76.3° between the two ligand planes.[18] Both the propentdyopent anion and the tetramethyldipyrromethane anion have similar geometries and properties. Both act as planar ligands. The bulk of the oxygen atoms in the propentdyopent and the 5,5′ methyl substituents of the dipyrromethane prohibit the two ligands in bischelate complexes from becoming coplanar. Additionally, $Co^{II}(TEPD)_2 \cdot CH_2Cl_2$ and $Cu^{II}(TEPD)_2 \cdot CH_2Cl_2$ are isostructural.

Analysis of the Hydrogen Bonding Networks in Crystalline $Co^{II}(TEPD)_2$. The tab/slot hydrogen bonding scheme that was previously shown to occur in several complexes of octaethylbiliverdin[14,16a] is also utilized in the intermolecular

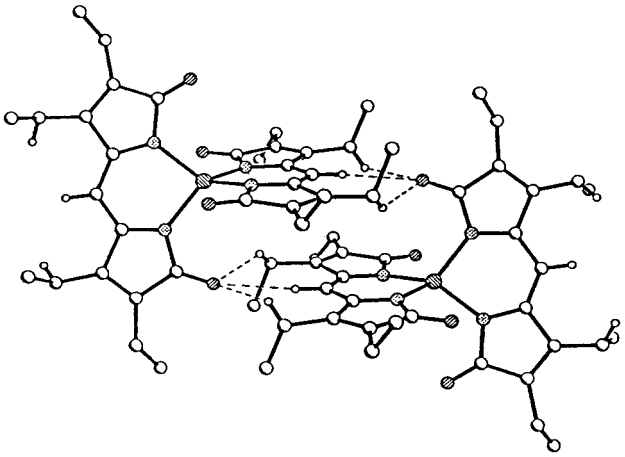

Figure 4. Representation of the hydrogen bonding interactions between $Co^{II}(TEPD)_2$ complexes.

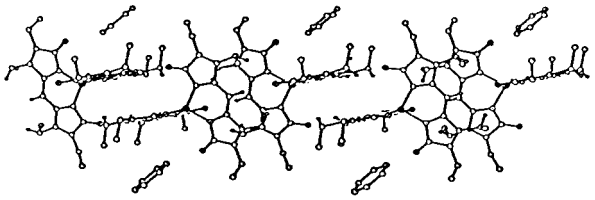

$Co^{II}(TEPD)_2 \cdot 0.5\ C_6H_6$

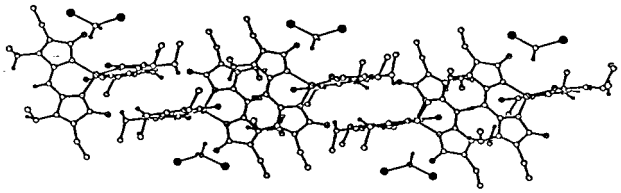

$Co^{II}(TEPD)_2 \cdot CH_2Cl_2$

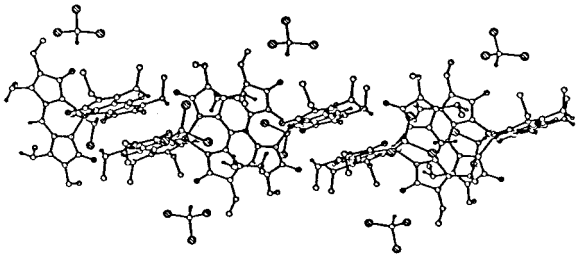

$Co^{II}(TEPD)_2 \cdot 2\ CHCl_3$

Figure 5. View of the intermolecular network of $Co^{II}(TEPD)_2$ molecules formed by hydrogen bonding between the keto oxygen atoms and methylene and meso hydrogen atoms in the three morphologies.

organization of all three crystalline forms of $Co^{II}(TEPD)_2$. This tab/slot arrangement involves hydrogen bonding between the lactam oxygen atoms and three C−H groups: the meso C−H group and methylene C−H groups on the two flanking ethyl groups as seen in Figure 4. Figure 5 shows the chains of $Co^{II}(TEPD)_2$ molecules that form in the solid. Each molecule of $Co^{II}(TEPD)_2$ is involved in two of the tab/slot arrangements shown in Figure 4. Additionally, the solvate molecules lie near the lactam oxygen atoms and form an additional C−H···O hydrogen bond in this fashion. The distances between the atoms

(18) Cotton, F. A.; DeBoer, B. G.; Pipal, J. R. *Inorg. Chem.* **1970**, *9*, 783.

Table 2. Intermolecular Hydrogen Bonding Distances (Å) and Angles (deg)

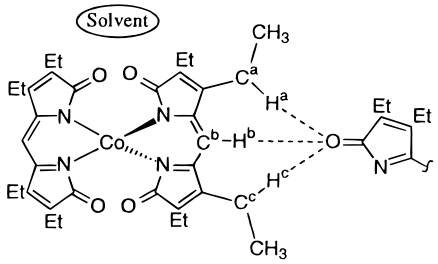

	$Co^{II}(TEPD)_2 \cdot 0.5C_6H_6$	$Co^{II}(TEPD)_2 \cdot CH_2Cl_2$	$Co^{II}(TEPD)_2 \cdot 2CHCl_3$	$Cu^{II}(TEPD)_2 \cdot 2CH_2Cl_2$
distances (Å)				
O···H^a	2.585, 2.537	2.558	2.479, 2.537	2.539
O···H^b	2.502, 2.527	2.537	2.504, 2.619	2.490
O···H^c	2.523, 2.647	2.601	2.542, 2.572	2.511
O···C^a	3.343, 3.255	3.368	3.289, 3.333	3.332
O···C^b	3.460, 3.486	3.503	3.445, 3.556	3.439
O···C^c	3.266, 3.363	3.353	3.361, 3.431	3.368
solvent-H···O	2.864, 2.949	*a*	2.201, 2.127	2.13, 2.20
solvent-C···O	3.465	*a*	3.032, 3.153	3.367
angles (deg)				
O−H^a−C^a	136.0, 131.6	138.9	138.8, 141.0	139.9
O−H^b−C^b	176.1, 175.8	174.8	170.6, 168.9	170.1
O−H^c−C^c	134.2, 131.7	138.8	140.0, 145.1	148.7

[a] Measurement precluded due to solvent disorder.

that are involved in these C−H···O hydrogen bonding interactions are given in Table 2. The distances are consistent with other examples of C−H···O hydrogen bonds which have received considerable attention recently.[19] The formation of the extensive scheme of hydrogen bonding interactions shown in Figure 5 stabilizes the solid and contributes to the relatively low solubility of this molecule. Additionally $Cu^{II}(TEPD)_2 \cdot CH_2Cl_2$, which is isomorphic with $Co^{II}(TEPD)_2 \cdot CH_2Cl_2$, also participates in the tab/slot hydrogen bonding scheme that is shown in Figure 5.

Electrochemical Studies of $Co^{II}(TEPD)_2$. The cyclic (CV) and Osteryoung square wave (OSWV) voltammograms of $Co^{II}(TEPD)_2$ in dioxygen-free methylene chloride and pyridine solutions have been recorded. Traces A and B of Figure 6 show the CV and OSWV voltammograms of $Co^{II}(TEPD)_2$ in dioxygen-free methylene chloride. The two reduction waves ($E_f°$, vs [Fc/Fc$^+$]: −1162 mV, −1355 mV) are indicative of reversible, one-electron processes (ΔE_p: 57 mV, 56 mV). The dioxygen-free pyridine solution the complex shows nearly identical redox behavior with two one-electron, reversible reduction waves (ΔE_p: 57 mV, 57 mV) at −1143 mV and −1381 mV ($E_f°$, vs [Fc/Fc$^+$]) indicating that pyridine coordination to $Co^{II}(TEPD)_2$ and $[Co(TEPD)_2]^-$ does not occur.

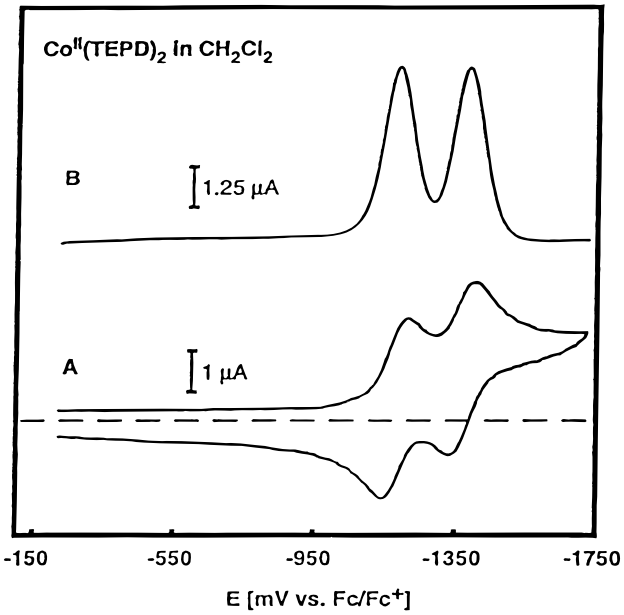

Figure 6. (A) Cyclic and (B) Osteryoung square wave voltammograms of $Co^{II}(TEPD)_2$ in dioxygen-free dichloromethane. The sample concentration is 1.1 mM with 0.1 M tetrabutylammonium perchlorate as the supporting electrolyte. The dashed line represents the zero of current.

Discussion

This work demonstrates that $Co^{II}(TEPD)_2$ is readily formed from the four cobalt tetrapyrrole precursors as shown in Scheme 2. The methine carbon and formyl carbon atoms that are excised in the thermal form of these reactions may be the source of the carbon monoxide and carbon dioxide which have been identified in the gas phase above the reaction media. The facile formation of the propentdyopent groups from chelated tetrapyrroles (e.g., Co(OEB) and Cu(OEB)) gives a direct route from the open chain tetrapyrrole to the propentdyopent. These results indicate that the failure to detect biliverdin as a product of the biological reactions such as those shown in Scheme 1 does not exclude it as an intermediate in propentdyopent formation, since biliverdin or its chelated from may undergo further oxidation as is the case in the present study.

The mechanisms involved in the oxidative reactions shown in Scheme 2 are far from clear. The thermal conversions of Co(OEB), $[Co^{II}(OEBOx)]I_3$, and $Co^{II}(OEB-OMe)$ to $Co^{II}(TEPD)_2$ seem to be related to the types of reactions that occur during heme degradation via either heme oxidase or coupled oxidation.[7] However, the low yields of these thermal paths do not present attractive experimental targets for detailed mechanistic investigations at this point. In the conversion of $Co^{II}(OEFB)$ to $Co^{II}(TEPD)_2$, the relatively high yield in the

(19) (a) Taylor, R.; Kennard, O. *J. Am. Chem. Soc.* **1982**, *104*, 5063. (b) Desiraju, G. R. *Acc. Chem. Res.* **1991**, *24*, 290. (c) Pedireddi, V. R.; Desiraju, G. R. *J. Chem. Soc., Chem. Commun.* **1992**, 988.

Table 3. Crystal Data and Data Collection Parameters for $Co^{II}((TEPD)_2 \cdot 0.5C_6H_6$, $Co^{II}((TEPD)_2 \cdot CH_2Cl_2$, and $Co^{II}((TEPD)_2 \cdot 2CHCl_3$

	$Co^{II}(TEPD)_2 \cdot 0.5C_6H_6$	$Co^{II}(TEPD)_2 \cdot CH_2Cl_2$	$Co^{II}(TEPD)_2 \cdot 2CHCl_3$
empirical formula	$C_{37}H_{45}CoN_4O_4$	$C_{35}H_{44}Cl_2CoN_4O_4$	$C_{36}H_{44}Cl_6CoN_4O_4$
fw	688.70	714.57	868.38
color and habit	red parallele-piped	purple block	brown plate
cryst syst	triclinic	monoclinic	triclinic
space group	$P\bar{1}$	$C2/c$	$P\bar{1}$
a, Å	11.197(3)	17.426(4)	12.399(3)
b, Å	11.703(3)	13.921(3)	14.181(4)
c, Å	14.754(4)	14.981(3)	14.193(4)
α, deg	92.37(2)	90	75.78(2)
β, deg	105.30(2)	103.05(3)	64.70(2)
γ, deg	110.42(2)	90	67.22(2)
V, Å^3	1728.5(8)	3540.3(12)	2070.6(10)
Z	2	4	2
T, K	130(2)	133(2)	130(2)
d_{calcd}, g cm^{-3}	1.285	1.341	1.393
radiation (λ, Å)	Mo Kα (0.710 73)	Mo Kα (0.710 73)	Mo Kα (0.710 73)
μ, mm^{-1}	0.541	0.678	0.843
range of transm factors	0.77−0.84	0.89−0.93	0.89−0.96
R1[a]	0.048	0.070	0.086
wR2[b]	0.110	0.149	0.181

[a] $R1 = \sum||F_o| - |F_c||/\sum|F_o|$. [b] $wR2 = [\sum[w(F_o^2 - F_c^2)^2]/\sum[w(F_o^2)^2]]^{1/2}$.

photochemical reaction suggests that both the formyl group and the central methine group in Co^{II}(OEFB) undergo oxidative cleavage. Photochemical oxidations of zinc and magnesium porphyrins have been suggested to occur via 2 + 2 cycloadditions of dioxygen to the porphyrin C(methine)−C(pyrrole) bond.[20] Such reactions may initiate the transformations of the tetrapyrrole complexes that eventually lead to the production of $Co^{II}(TEPD)_2$. However, the reactivities observed in the reactions shown in Scheme 2 are more complex and require additional C−C bond cleaving steps.

Outside of this laboratory, the propentdyopent ligand has received little study in the formation of coordination compounds, although a zinc compound was reported previously.[4a,5a] The geometric properties of this ligand are similar to those of 3,3′,5,5′-tetramethyldipyrromethane.[18] For both, the position of the oxygen atoms or the 3,3′ methyl groups offer steric restrictions that will favor nonplanar geometry in bischelate complexes. These steric factors also appear to be partially responsible for the observations that $Co^{II}(TEPD)_2$ does not add additional ligands such as pyridine and carbon monoxide.

While the three X-ray crystal structures of $Co^{II}(TEPD)_2$ show nonorthogonal propentdyopent ligand planes, the lack of diasteriotopic methylene resonances in the ^{1}H NMR spectrum indicates that this complex has approximate D_{2d} symmetry in solution or rapidly interconverts between the two enantiomeric D_2 forms on the NMR time scale. The nonorthogonal arrangements of the propentdyopent ligands, which are modulated by the presence of different solvate molecules, can be attributed, in part, to intermolecular interactions.

Since the ligand itself is redox active, it is not surprising that $Co^{II}(TEPD)_2$ undergoes one-electron redox processes. The electrochemical data presented in Figure 6 indicate that this complex is a member of a three-part, electron-transfer series that includes $[Co(TEPD)_2]^n$ where n may be 0, −1, or −2.

Experimental Section

Preparation of Compounds. $Co^{II}(TEPD)_2$. Co^{II}(OEFB)[14] (27 mg, 0.043 mmol) was dissolved in 75 mL of benzene and placed in a quartz photolysis tube. The solution and tube were flushed with dioxygen gas for 1 min, sealed, and irradiated with UV light for 3.5 h while maintained at room temperature. The resulting brown-red solution was concentrated to ca. 10 mL under reduced pressure and a layer of *n*-hexane was added over the solution. After 18 h, crystalline $Co^{II}(TEPD)_2$ was collected by filtration, washed with methanol, and dried under vacuum: yield 18 mg, 66%. A similar reaction that utilized Co(OEB)[15] instead of Co^{II}(OEFB) produced $Co^{II}(TEPD)_2$ in 9% yield. $Co^{II}(TEPD)_2$ may also be produced by heating a toluene solution of Co^{II}(OEFB) at 90 °C under a dioxygen atmosphere for 24 h. The yield by this method is much lower (ca. 10%). A toluene solution of Co(OEB) (10.4 mg, 0.017 mmol) heated to 90 °C under a dioxygen atmosphere for 46 h produced $Co^{II}(TEPD)_2$ in 16% yield. EI-MS m/z (relative intensity): 629.26 (100) M^+.

X-ray Data Collection. For each data collection, a suitable crystal was coated with a light hydrocarbon oil and mounted in the ca. 130 K dinitrogen stream of a Siemens R3m/V diffractometer that was equipped with a low-temperature device. During the three separate data collections, two check reflections showed less than 2% decay during the data collection. Crystal data are given in Table 3. Each data set was corrected for Lorentz and polarization effects. Following data collection for $Co^{II}(TEPD)_2 \cdot 0.5C_6H_6$, the crystal was dissolved in a minimal volume of chloroform-*d* and spectroscopic data were collected for that solution. The ^{1}H NMR spectrum and the UV−vis spectrum of this solution were identical to spectra gathered from the bulk sample of this complex.

Solution and Refinement. Calculations were performed with the SHELXTL v5.03 suite of programs for all three morphologies of $Co^{II}(TEPD)_2$. Scattering factors for neutral atoms and corrections for anomalous dispersion were taken from a standard source.[21] An absorption correction was applied to each data set.[22] The initial solution of the structure was obtained by direct methods for $Co^{II}(TEPD)_2 \cdot 0.5C_6H_6$ and $Co^{II}(TEPD)_2 \cdot 2CHCL_3$. Isomorphic replacement, using previously published crystallographic data for $Cu(TEPD)_2 \cdot CH_2Cl_2$, was used for the initial solution of $Co^{II}(TEPD)_2 \cdot CH_2Cl_2$. For all three structures, hydrogen atoms were found on a difference map and refined at ideal geometries.

$Co^{II}(TEPD)_2 \cdot 0.5C_6H_6$. The complex crystallizes in the triclinic space group $P\bar{1}$ with a complete $Co^{II}(TEPD)_2$ molecular unit and half of a benzene molecule in the asymmetric unit. The centroid of the benzene solvate lies on a center of symmetry. The structure shows disorder in the position of the methyl carbon, C(34). This was modeled with the disordered methyl group situated in two sites, C(34) and C(34A) (see Figure S1) with occupancies which refined to 0.82 and 0.18, respectively.

(20) Wasser, P. K. W.; Fuhrhop, J.-H. *Ann. N.Y. Acad. Sci.* **1973**, *206*, 533.
(21) *International Tables for X-ray Crystallography*; Kynoch Press: Birmingham, England, 1974; Vol. 4.
(22) Parkins, S.; Moezzi, B.; Hope, H. *J. Appl. Crystallogr.* **1995**, *28*, 53.

$Co^{II}(TEPD)_2 \cdot CH_2Cl_2$. Half of the $Co^{II}(TEPD)_2$ molecule and a disordered dichloromethane molecule are present in the asymmetric unit. The dichloromethane molecule is disordered over two sites (see Figure S2). One molecule, C(18) and Cl(1), has a site occupancy of 0.20 and lies on a 2-fold rotation axis. Hydrogen atoms could not be modeled for this molecule. The second site consists of C(19), H(19), Cl(2), and Cl(3) and has a site occupancy of 0.30. Atoms C(18) and C(19) are separated by 0.504 Å. The chlorine atoms in each molecule were refined with a fixed Cl−Cl distance of 2.89 Å, while the C−Cl distances were fixed at 1.77 Å.

$Co^{II}(TEPD)_2 \cdot 2CHCl_3$. The asymmetric unit contains a complete $Co^{II}(TEPD)_2$ molecular unit and two disordered chloroform molecules (see Figure S3). One of the disordered chloroform molecules has two sets of chlorine atoms, {Cl(1A), Cl(2A), Cl(3A)} and {Cl(1B), Cl(2B), Cl(3B)} a common carbon, C(35), and H(35) whose location was calculated from the idealized position calculated from the two sets of chlorine atom positions. The thermal parameters for the chlorine atoms in sets A and B were kept equal and the relative occupancies of these two sites refined to 0.376(13) and 0.624(13), respectively. The second disordered chloroform molecule has three sets of chlorine atoms. The method of structure analysis was essentially the same as above with sets A, B, and C producing refined occupancies of 0.530(4), 0.242(4), and 0.229(4), respectively.

Instrumentation. ^1H NMR spectra were recorded on a General Electric QE−300 FT NMR operating in the quadrature mode (^1H frequency is 300 MHz). Typical spectra were collected over a 30 kHz spectral window with 8 K complex points, 256−2048 transients, and a repetition rate of 2.5 transients/s. The signal-to-noise ratio was improved by apodization of the free induction decay. The residual ^1H resonances of the deuterated solvents were used as a reference.

Electrochemical measurements were recorded on a BioAnalytical Systems CV-50W potentiostat. All measurements were conducted at room temperature under an argon atmosphere using 0.1 M tetrabutylammonium perchlorate as the supporting electrolyte, a gold disc (0.75 mm radius) working electrode, Ag/Ag^+ reference electrode and a platinum foil auxiliary electrode. Cyclic voltammograms were collected with a 100 mV/s sweep rate. Osteryoung square wave voltammograms were collected using a 25 mV sweep width amplitude, 15 Hz sweep width frequency, 4 mV step potential, and a 2 s quiet time. Absorption spectra were recorded on a Hewlett-Packard 8452A diode array spectrophotometer. High-resolution EI (70 eV) mass spectrometry was performed on a VG Analytical ZAB-2F−HS mass spectrometer. Magnetic susceptibilities were determined by the Evans' technique.[23]

Acknowledgment. We thank the National Institutes of Health (GM-26226) for financial support and Dr. K. N. Brown and Dr. S. Attar for experimental assistance.

Supporting Information Available: Tables listing crystal data, atomic coordinates, isotropic and anisotropic displacement parameters, and bond lengths and bond angles for $Co^{II}(TEPD)_2 \cdot 0.5C_6H_6$, $Co^{II}(TEPD)_2 \cdot CH_2Cl_2$, and $Co^{II}(TEPD)_2 \cdot 2CHCl_3$ (33 pages). Ordering information is given on any current masthead page.

IC971265Q

(23) Evans, D. F.; James, T. A. *J. Chem. Soc., Dalton Trans.* **1979**, 723.